Functional Role of Transmembrane Helix 6 in Drug Binding and Transport by the ABC Transporter MsbA[†]

Barbara Woebking,[‡] Saroj Velamakanni,[‡] Luca Federici,[§] Markus A. Seeger,[‡] Satoshi Murakami,[||] and Hendrik W. van Veen*[,‡]

Department of Pharmacology, University of Cambridge, Cambridge, United Kingdom, Ce.S.I. Centro Studi sull'Invecchiamento, Fondazione Universita' "G. D'Annunzio", Dipartimento di Scienze Biomediche, Universita' di Chieti "G. D'Annunzio", Chieti, Italy, and Graduate School of Bioscience and Biotechnology, Tokyo Institute of Technology, Yokohama, Japan

Received May 1, 2008; Revised Manuscript Received June 27, 2008

ABSTRACT: The ATP-binding cassette transporter MsbA in Gram-negative bacteria can transport antibiotics and toxic ions. However, the key functional regions in MsbA which determine substrate specificity remain to be identified. We recently examined published mutations in the human MsbA homologue ABCB1 that alter multidrug transport in cells and identified mutations that affect the specificity for individual substrates (termed change-in-specificity mutations). When superimposed on the corrected 3.7 Å resolution crystal structure of homodimeric MsbA from S*almonella typhimurium*, these change-in-specificity mutations colocalize in a major groove in each of the two "wings" of transmembrane helices (TMHs) that point away from one another toward the periplasm. Near the apex of the groove, the periplasmic side of TMH 6 in both monomers contains a hotspot of change-in-specificity mutations and residues which, when replaced with cysteines in ABCB1, covalently interact with thiol-reactive drug analogues. We tested the importance of this region of TMH 6 for drug−protein interactions in *Escherichia coli* MsbA. In particular, we focused on conserved S289 and S290 residues in the hotspot. Their simultaneous replacement with alanine (termed the SASA mutant) significantly reduced the level of binding and transport of ethidium and Taxol by MsbA, whereas the interactions with Hoechst 33342 and erythromycin remained unaffected. Hence, the SASA mutation is associated with a change-in-specificity phenotype analogous to that of the change-in-specificity mutations in ABCB1. This study demonstrates for the first time the significance of TMH 6 for drug binding and transport by MsbA. Based on these data, a possible mechanism for alternating access of drug-binding surfaces in MsbA is discussed.

ATP-binding cassette (ABC)[1] transporters are integral membrane proteins that utilize the energy generated from ATP binding and hydrolysis to translocate a wide variety of molecules (e.g., lipids, polysaccharides, proteins, and small nutrients) across cellular membranes. These molecular pumps are found in all phyla and form one of the largest protein families (*1, 2*).

MsbA is an essential ABC transporter in Gram-negative bacteria, including the pathogens *Salmonella typhimurium*, *Vibrio cholera*, and *Pseudomonas fluorescence* (*3*). The transporter is involved in the transport of lipid A (also termed endotoxin) (*3, 4*), which is the lipid anchor of lipopolysaccharides in the outer membrane, and which is a potent activator of innate immunity in mammals via Toll-like receptors. MsbA can also extrude antibiotics and toxic ions from the cell (*5–8*). In a recent study of the kinetics of drug and lipid A binding and transport by MsbA from *Escherichia coli*, we found that these substrates can interact with MsbA with a comparable affinity and that lipid A binding can inhibit drug binding (*6*).

Our knowledge of the functional regions in MsbA or other bacterial ABC multidrug transporters affecting their substrate specificities is still limited. In contrast, a large body of data on amino acid replacements that influence the recognition and transport of drugs by the human MsbA homologue ABCB1 exists (reviewed in ref *9*). In a recent analysis of the reported mutations in ABCB1, we separated true change-in-specificity mutations, which affect the specificity for individual substrates, from those that either modify the expression of the protein at the cell surface or alter the overall transport mechanism, both determined by a comparable change in the transport of all substrates tested (*9*). Due to the absence of a high-resolution crystal structure of ABCB1, little information about the spatial arrangement of the change-in-specificity mutations is available, which could give insights into the location of drug binding sites in the protein.

Here, we superimposed the change-in-specificity mutations in ABCB1 on the recently determined high-resolution (3.7 Å resolution) crystallographic structure of homodimeric MsbA from *S. typhimurium* (*10*) (PDB accession number 3b60), the overall shape and domain organization of which

[†] This research was funded by the Biotechnology and Biological Sciences Research Council (BBSRC). M.A.S. is the recipient of a long-term EMBO fellowship. Collaborative work between H.W.V.V. and S.M. is supported by a Cooperative Research Project Award from the Japan Science and Technology Agency.

* To whom correspondence should be addressed. Telephone: +44-1223-765295. Fax: +44-1223-334100. E-mail: hwv20@cam.ac.uk.

[‡] University of Cambridge.

[§] Universita' di Chieti "G. D'Annunzio".

[||] Tokyo Institute of Technology.

[1] Abbreviations: ABC, ATP-binding cassette; MD, membrane domain; NBD, nucleotide-binding domain; μ_m, maximum specific growth rate; TMH, transmembrane helix.

10.1021/bi800778d CCC: $40.75
Published on Web 09/20/2008

resemble those of the 3.0 Å structure of the homodimeric ABC transporter Sav1866 from *Staphylococcus aureus* (*11*), and the 8 Å cryo-EM structure of ABCB1 (*12*) in which two MsbA-like units are covalently linked. As recent work on *E. coli* MsbA demonstrated that this protein can bind and transport multiple ABCB1 substrates (*5, 6, 8*), we tested the relevance of our structural comparisons of ABCB1 versus *S. typhimurium* MsbA for drug binding and transport by MsbA in a site-directed mutagenesis approach in which we substituted residues in a hotspot of change-in-specificity mutations in transmembrane helix (TMH) 6 of *E. coli* MsbA. This is the first report to demonstrate that TMH 6 in MsbA is an important determinant of specificity for individual substrates.

EXPERIMENTAL PROCEDURES

Construction of Plasmids. To generate mutant forms of *E. coli* MsbA, the *msbA* gene was subcloned from pNZMsbA (*6*) into the pGEM-5Zf(+) plasmid (Promega) using NcoI/XbaI sites, yielding pGEMMsbA. Site-directed mutagenesis on pGEMMsbA was performed using QuikChange (Stratagene, Amsterdam, The Netherlands) with the forward primer, 5′-CCG TTG TTT TCG CTG CAA TGA TTG CAC TGA TGC-3′ and the reverse primer, 5′-GCA ATC ATT GCA GCG AAA ACA ACG GTA ATC GTA CC-3′ to give pGEMMsbA-S289A S290A and the forward primer 5′-CGG GTT CAA CCA TCG CCA GCC TG-3′ and the reverse primer 5′-TGG TTG AAC CCG AAC CAG AGC GTC C-3′ to give pGEMMsbA ΔK382. The PCR products were digested with NcoI/XbaI (Roche Applied Science, Herts, U.K.) and ligated into lactococcal vector pNZ8048 (*13*) under the control of the nisin A-inducible promoter *nisA*, yielding pNZMsbA ΔK382 and pNZMsbA S289A S290A. The genes were sequenced to ensure that only the intended mutation had been introduced.

Growth of Cells. Lactococcus lactis NZ9000 Δ*lmrA* Δ*lmrCD* (*14, 15*) was grown at 30 °C in M17 medium (Difco) supplemented with 20 mM glucose and 5 μg/mL chloramphenicol to an A_{660} of 0.3. Unless indicated otherwise, for protein expression, cells harboring pNZMsbA, pNZMsbA S289A S290A, pNZMsbA ΔK382, or pNZ8048 were incubated for 2 h at 30 °C in the presence of a 1:1000 dilution of the culture supernatant of nisin A-producing *L. lactis* strain NZ9700 (*13*), corresponding to a nisin A concentration of approximately 10 pg/mL (*16*).

For cytotoxicity experiments, cells were grown at 30 °C to an A_{660} of 0.3. Subsequently, protein expression was induced by the addition of 1 pg/mL nisin A preceding the start of the measurements. The cells were dispensed in the wells of a 96-well plate in the presence of a range of concentrations of drugs. Growth was monitored at 30 °C by measuring the A_{660} every 15 min for 5 h in a Versamax plate reader (Molecular Devices). The 50% inhibitory concentration (IC_{50}) was then determined as the concentration of drug that reduces the maximum specific growth rate by 50%.

Preparation of Inside-Out Membrane Vesicles. Lactococcal cells were grown to an A_{660} of 0.5 and incubated for 1 h at 30 °C in the presence of nisin A to induce protein expression. Cells were harvested by centrifugation at 13000*g* for 15 min. The cell pellet was washed at 4 °C in 50 mM potassium phosphate buffer (pH 7.0), resuspended to an A_{660} of 40 in potassium phosphate buffer containing 2 mg/mL lysozyme and complete protease inhibitor mixture (Roche Applied Science), and incubated for 30 min at 30 °C. Cells were broken by being passed three times through a Basic Z 0.75-kW Benchtop Cell Disruptor at 20000 psi. The solution was incubated at 30 °C for 30 min after addition of $MgSO_4$ and DNase to final concentrations of 1 mM and 10 μg/mL, respectively. K-EDTA (pH 7.0) was then added to a final concentration of 15 mM to prevent aggregation of the membranes. Unbroken cells and cell debris were removed by centrifugation at 13000*g* for 15 min at 4 °C. Inside-out membrane vesicles were harvested by centrifugation at 125000*g* for 50 min at 4 °C. The membrane vesicles were resuspended in 100 mM potassium phosphate buffer (pH 7.0) containing 10% (v/v) glycerol and were stored in 200 μL aliquots in liquid N_2.

Purification of the His_6-Tagged Protein. Inside-out membrane vesicles were solubilized by rotation at 4 °C for 3 h in solubilization buffer [50 mM potassium phosphate (pH 8.0) containing 10% (v/v) glycerol, 0.1 M NaCl, and 1% (w/v) *n*-dodecyl β-D-maltoside]. The mixture was centrifuged at 125000*g* for 30 min to remove unsolubilized components. The solubilized protein was mixed with Ni^{2+}-nitrilotriacetic acid resin suspension (Qiagen, West Sussex, U.K.), which had been preequilibrated with wash buffer A [50 mM potassium phosphate (pH 8.0) containing 10% (v/v) glycerol, 20 mM imidazole, 0.1 M NaCl, and 0.05% (w/v) *n*-dodecyl β-D-maltoside], at a ratio of 10 mg of His_6-tagged protein/mL of resin. The resin was then transferred to a 2 mL volume Biospin disposable chromatography column (Bio-Rad). After subsequent washing with 4 volumes of wash buffer A and 7 volumes of wash buffer B [50 mM potassium phosphate (pH 7.0) containing 10% (v/v) glycerol, 20 mM imidazole, 0.1 M NaCl, and 0.05% (w/v) *n*-dodecyl β-D-maltoside], the protein was eluted with 5 volumes of elution buffer [50 mM potassium phosphate (pH 7.0) containing 5% (v/v) glycerol, 150 mM imidazole, 0.1 M NaCl, and 0.05% (w/v) *n*-dodecyl β-D-maltoside]. Total purified protein was assayed using the colorimetric DC protein assay (Bio-Rad, Hertfordshire, U.K.) at A_{750}.

ATPase Activity Measurements. ATPase activities of purified MsbA proteins were determined using an enzymatic assay in which ATP hydrolysis is coupled to NADH oxidation. To measure basal ATPase activity, the reaction buffer [50 mM K-HEPES (pH 8.0) containing 0.3 mM NADH, 4 mM phosphoenolpyruvate (Roche), 50 μg/mL pyruvate kinase, 10 μg/mL lactate dehydrogenase (Roche), 3.3 mM $MgCl_2$, and 3.3 mM ATP] was equilibrated at 30 °C for 5 min. The reaction was started by the addition of 3 μg/mL purified protein in elution buffer or the same volume of elution buffer without protein as a control, and the A_{340} was monitored for 30 min at 30 °C in a VersaMax microplate reader. An NADH standard curve with a range of NADH concentrations between 0 and 300 μM was measured in the same buffer. To measure the drug-stimulated ATPase activity, the drugs were added to the reaction buffer before the addition of protein. The lack of an effect of drugs on the enzymes in the coupled assay was confirmed in control experiments in which ADP was included instead of ATP.

Equilibrium Binding of [^{14}C]Taxol. For equilibrium binding of Taxol to MsbA, inside-out membrane vesicles (0.5 mg of membrane protein) in 100 μL of 50 mM Tris-HCl (pH 7.4) were incubated as described previously (*17*) for 2 h at 20 °C in the dark in the presence of 1 μM ^{14}C-labeled Taxol {[2-benzoyl ring-^{14}C(U)]Taxol in ethanol} (73 mCi/mmol, Moravek Biochemicals) and unlabeled Taxol in the range of 0−40 μM. A period of 2 h was sufficient to obtain steady-state binding of Taxol (not shown). After the incubation period, MsbA was stable in the solution for an additional period of at least 2 h, as determined in an ultracentrifugation dispersity sedimentation assay (*18*). The binding assay was terminated by the addition of 3 mL of ice-cold 20 mM Tris-HCl (pH 7.4) containing 20 mM $MgSO_4$ (wash buffer). Samples were immediately filtered through Whatman GF/B glass fiber filters that had been preequilibrated overnight at 4 °C in wash buffer. The filters were washed twice with 3 mL of ice-cold wash buffer, and filter-retained radioactivity was measured by liquid scintillation counting using the scintillant Ultima Gold XR (Perkin-Elmer Life Sciences). Nonspecific binding (usually <40% of total binding) was defined as the amount of [^{14}C]Taxol bound to control vesicles without MsbA containing the non-Taxol binding galactoside transporter GalP (expressed at a level similar to that of MsbA) (*19, 20*) and was subtracted.

Transport of [^{14}C]Taxol. Intact cells expressing wild-type (Wt) or mutant MsbA and nonexpressing control cells were grown to an A_{660} of 0.6, and protein expression was induced for 1 h at 30 °C. The cells were harvested by centrifugation at 6500*g* for 10 min at 4 °C and washed once in 50 mM ice-cold potassium phosphate (pH 7.0). The cells were deenergized in the presence of the uncoupler 2,4-dinitrophenol (0.5 mM) and washed three times with 50 mM ice-cold potassium phosphate buffer (pH 7.0) containing 5 mM $MgSO_4$. The cells were resuspended to an A_{660} of 5 and kept on ice until needed. After a 1:10 dilution in the same buffer, the cells were incubated at 20 °C in the presence of 25 μM [^{14}C]Taxol (3.7 mCi/mmol) for 30 min under mild stirring. Where required, 25 mM glucose was added, and samples of 200 μL were rapidly filtered over Whatman GF/B glass fiber filters, which were preequilibrated overnight at 4 °C in 50 mM potassium phosphate buffer (pH 7.0). The filters were washed twice with 3 mL of ice-cold potassium phosphate buffer. The radioactivity retained on the filters was measured by liquid scintillation counting using Ultima Gold XR counting scintillant. All data were corrected by subtracting nonspecific binding to the filters, which was usually <0.1% of the total radioactivity count.

Ethidium Transport. For measurement of ethidium efflux, cells were ATP-depleted as described for Taxol transport. Control cells and cells containing Wt or mutant MsbA were preloaded with 2 μM ethidium at 30 °C until a steady-state level was reached (approximately 20 min for cells expressing Wt or mutant MsbA and approximately 40 min for control cells). Subsequently, 25 mM glucose was added to the cells as a source of metabolic energy, after which the ethidium fluorescence was monitored. To measure facilitated ethidium uptake by MsbA in cells, ATP-depleted cells were diluted 1:10 in 2 mL of buffer to a final A_{660} of 0.5, and uptake was started with the addition of ethidium. When required, Taxol (in ethanol) was added with a final concentration of ethanol below 1.0% (v/v). Samples without Taxol received the solvent only. Ethidium fluorescence was measured in an LS-55B luminescence spectrometer (Perkin-Elmer) at excitation and emission wavelengths of 500 and 580 nm, respectively, and slit widths of 5 and 10 nm, respectively.

Ethidium Fluorescence Anisotropy Measurements. Binding of ethidium to purified protein was assessed by fluorescence anisotropy as described previously (*19*) at a concentration of 1 μM ethidium in 2 mL of 50 mM potassium phosphate buffer (pH 7.0). The fluorescence anisotropy in the solution was measured in an LS-55B luminescence spectrometer at excitation and emission wavelengths of 500 and 580 nm, respectively, with slit widths of 10 nm each. The grating factor was calculated for each addition, and the anisotropy was measured 1 min after each addition of protein for 1 min with an integration time of 1 s. Purified protein was diluted to a concentration of 400 μg/mL and was added to the ethidium solution in a stepwise fashion to a final concentration of 34 μg/mL, where no major changes in anisotropy values were observed. Half-molar amounts of the purified 12-TMH-containing proton/galactose symporter GalP were used as a control for nonspecific binding to the membrane domain of MsbA (*19, 20*), and the values obtained were subtracted from the anisotropy readings obtained for MsbA proteins.

Kinetic Analysis of Hoechst 33342 Transport. Inside-out membrane vesicles (250 μg of total protein) were diluted into 2 mL of 100 mM potassium phosphate buffer (pH 7.0) containing 5 mM $MgSO_4$, 0.1 mg/mL creatine kinase, and 5 mM phosphocreatine (both Roche). The trace was followed in the fluorimeter (excitation and emission wavelengths of 355 and 457 nm, respectively, and slit widths of 10 and 5 nm, respectively) for 50 s. Hoechst 33342 (0.25 μM) was then added, and the fluorescence was monitored until a steady state was reached. Subsequently, sodium ATP [in 50 mM potassium phosphate (pH 7.0)] was added to a final concentration 1 mM, and the fluorescence intensity was recorded for an additional 200 s. When the effect of Taxol on Hoechst 33342 transport was tested in this assay, the Taxol or its solvent ethanol [<1% (v/v)] was added just before the addition of Hoechst 33342.

Hoechst 33342 Binding to Purified MsbA. Hoechst 33342 binding to purified protein was carried out in 2 mL reaction mixtures containing 10 μg of purified protein in 100 mM potassium phosphate (pH 7.0). Hoechst 33342 was added to the solution in a stepwise fashion to a final concentration of 1.5 μM, when no major changes in fluorescence were detected. For the assessment of Hoechst 33342 binding in the presence of Taxol, the samples were incubated with 30 μM Taxol or its solvent [<1% (v/v) ethanol] for 5 min prior to the addition of Hoechst 33342. Measurements were performed in an LS-55B luminescence spectrometer at excitation and emission wavelengths of 355 and 457 nm, respectively, and slit widths of 5 and 10 nm, respectively.

Curve Fitting and Statistical Analyses. Transport data were fitted to the Michaelis−Menten equation, $V = V_{max}[S]/(K_m + [S])$, in which the rate of drug transport is represented by V, the drug concentration by [S], the maximal transport rate by V_{max}, and the drug concentration yielding $^1/_2V_{max}$ by the Michaelis constant (K_m). The binding constants B_{max} and K_d were determined using the relationship $B = B_{max}[S]/(K_d +$

[S]), in which drug binding is represented by B, the drug concentration by [S], the maximal binding by B_{max}, and the drug concentration yielding $^1/_2B_{max}$ by the dissociation constant K_d. Where appropriate, the binding data were fitted to a Hill equation, $B = B_{max}[S]^n/(K_d{}^n + [S]^n)$, in which $K_d = (K_d,1 \times K_d,2 \times ... \times K_d,n)^{1/n}$ is the average dissociation constant and n is the number of ligand binding sites in the ideal case of completely cooperative binding, which is estimated experimentally by the Hill number. From ethidium fluorescence anisotropy measurements, an apparent K_d was determined by fitting the data to the equation $A = A_{free} + [(A_{bound} - A_{free})[P]]/(K_d + [P])$, in which A is the measured change in ethidium fluorescence anisotropy, A_{bound} is the fluorescence anisotropy of ethidium bound to protein, A_{free} is the fluorescence anisotropy of the free ethidium, [P] is the protein concentration, and K_d is the dissociation constant (*21*). In cytotoxicity assays, the maximum specific growth rate μ_m was estimated from growth curves by fitting the data to the equation $N_t = N_0e^{\mu_m t}$, in which N_t and N_0 are the cell densities at times t and 0 h, respectively. All statistical analyses were based on four independent observations ($n = 4$), unless indicated otherwise, using different batches of cells or membrane vesicles. The statistical analyses were made using a Student's t test with a 95% confidence interval for the sample mean.

RESULTS

Superimposition of Change-In-Specificity Mutations in ABCB1 on Dimeric MsbA and Identification of SASA Mutation in MsbA. Superimposition of previously described change-in-specificity mutations in ABCB1 (*9*) on the crystal structure of dimeric MsbA from *S. typhimurium* (*10*) revealed that the mutations colocalize in a major groove in each of the two "wings", one of which is formed by TMH 1 and 2 of one half-transporter and TMH 3′, 4′, 5′, and 6′ of the other and the other wing is formed by the remainder of the TMHs (Figures 1 and 2). In this groove, TMH 5 (corresponding to TMH 11 in ABCB1) contains change-in-specificity mutations along its entire length, whereas in TMH 6 and TMH 6′ (corresponding to TMH 12 and TMH 6 in ABCB1, respectively), the change-in-specificity mutations are confined to a hotspot at the periplasmic side of the helix, near the apex of the groove (Figures 1B,C and 2A). In addition, this region of TMH 6 and TMH 6′ is rich in residues which, when replaced with cysteines in cysteine scanning mutagenesis experiments on ABCB1, were found to react with the thiol-reactive drug analogues methanethiosulfonate (MTS)-verapamil (*22*) and/or MTS-rhodamine (*23*) (Figures 1B,C and 2A). As the reactive cysteines could be specifically protected with unconjugated rhodamine or verapamil, these studies might indicate that these hotspot regions in TMH 6 and TMH 6′ contribute to a binding surface for these substrates.

To test the relevance of our analysis for drug binding and transport by MsbA, we identified two adjacent serine residues in the hotspot regions, S289 and S290 (Figures 1B,C and 2A), which are conserved in TMH 12 and TMH 6 of ABCB1, respectively (data not shown). We substituted both Ser residues with Ala, yielding the S289A S290A (SASA) MsbA mutant. The pharmacological properties of Wt MbA and the SASA mutant were compared in detail in drug-stimulated ATPase activity assays and measurements of drug binding and transport. For this purpose, MsbA proteins were expressed in *L. lactis* Δ*lmrA* Δ*lmrCD* (*14, 15*), which was previously used to study the properties of the ABC multidrug transporters LmrA and ABCG2 in the absence of endogenous multidrug transport activity (*15, 20*). Wt MsbA and the SASA mutant were expressed at a similar level in the cytoplasmic membrane of the lactococcal cells (data not shown).

Basal ATPase Activity of the SASA Mutant Is Not Stimulated by Taxol. The interaction of Taxol with MsbA proteins was first tested in ATPase measurements using purified Wt MsbA and SASA MsbA (Figure 3A). No significant differences could be detected between the basal ATPase activities for Wt MsbA and the SASA mutant [624 ± 28 and 692 ± 78 nmol of ATP min^{-1} (mg of protein)$^{-1}$, respectively]. Interestingly, while the ATPase activity of Wt MsbA could be stimulated 1.4-fold [to 835 ± 45 nmol of ATP min^{-1} (mg of protein)$^{-1}$] in the presence of 25 μM Taxol, this drug failed to significantly stimulate the ATPase activity of the SASA mutant [726 ± 110 nmol of ATP min^{-1} (mg of protein)$^{-1}$] (Figure 3A).

The Binding Affinity of SASA MsbA for Taxol Is Reduced. Equilibrium binding of [^{14}C]Taxol to MsbA was assessed by incubation of control inside-out membrane vesicles and membrane vesicles containing Wt or mutant MsbA in the presence of a range of Taxol concentrations. Subsequently, the samples were rapidly filtered, and the radioactivity retained on the filters was determined by liquid scintillation counting. After subtraction of nonspecific binding, the amount of the Taxol bound per milligram of protein was calculated and plotted against the free Taxol concentration. The data for Wt MsbA followed sigmoidal binding behavior (Figure 3B), and fitting of the data to the Hill equation yielded a B_{max} of 4.3 ± 1.2 nmol/mg of protein with an average K_d of 16.8 ± 1.7 μM and a Hill number (n) of 3.7 ± 0.5. For the SASA mutant, the binding curve was right-shifted due to a significant reduction in binding affinity, with a B_{max} of 4.9 ± 0.8 nmol/mg of protein, an average K_d of 39.9 ± 2.3 μM, and an n of 2.9 ± 0.8. These results indicate that the SASA mutant had a reduced binding affinity for Taxol compared to Wt MsbA and that the mutation altered the cooperativity between Taxol binding sites and/or the number of Taxol binding sites.

SASA MsbA Reduces the Rate of Taxol Transport. As the results for the Taxol-stimulated ATPase activity and equilibrium binding of [^{14}C]Taxol pointed to the inhibition of the interaction of the SASA mutant with Taxol, we also studied the transport of [^{14}C]Taxol by this mutant protein. ATP-depleted cells were preincubated with 25 μM Taxol for 30 min, after which glucose (25 mM) was added to allow the generation of metabolic energy (Figure 3C). While no major changes in cell-associated Taxol could be detected for control cells without MsbA expression throughout the experiment, cells expressing MsbA first accumulated Taxol and then extruded the Taxol when glucose was added, down to the level observed for the control. The SASA mutant exhibited a reduced rate of facilitated Taxol uptake compared to Wt MsbA (Figure 3C). Furthermore, the addition of glucose elicited active Taxol extrusion at a rate that was strongly reduced compared to that of Wt MsbA.

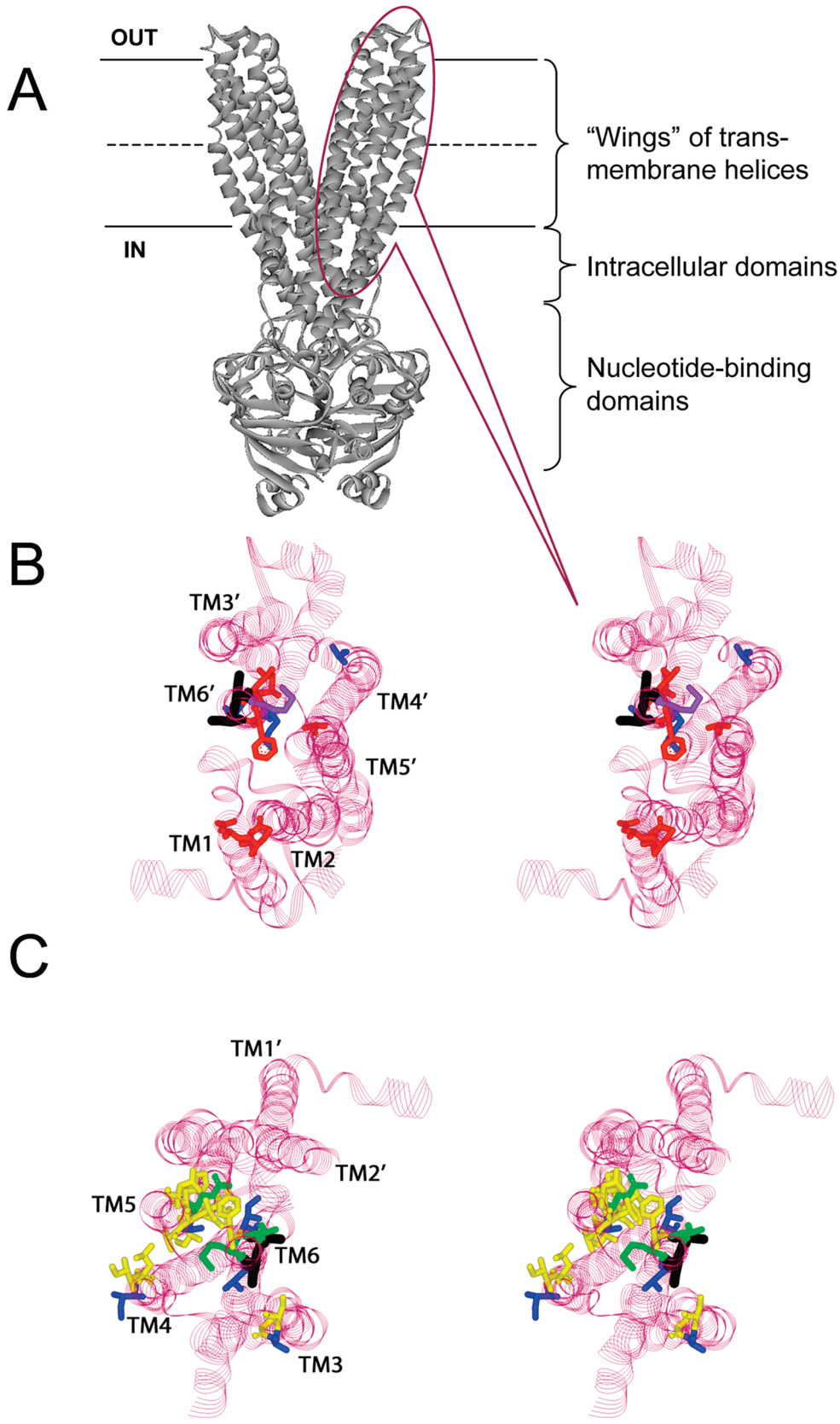

FIGURE 1: Residues implicated in drug binding by ABCB1 colocalize in the transmembrane-spanning wings of dimeric MsbA. (A) Ribbon representation of the crystal structure of homodimeric MsbA from *S. typhimurium* (*10*), which shares similarity with the structure of Sav1866 (*11*). (B and C) Stereoviews of the wings from the outside surface of the cytoplasmic membrane, obtained by −90° rotation about the *X*-axis of the side view in panel A. Shown are residues 10–110 (subunit A), 127–323 (subunit B) in (B) and residues 120–324 (subunit A), 10–112 (subunit B) in (C). Residues indicated are change-in-specificity mutations (red or yellow), residues accessible to thiol-reactive drug analogues (blue), and residues belonging to both classes (purple or green). TMHs 1′−6′ and 1−6 in dimeric MsbA (abbreviated as TMs in the Figure) refer to TMHs 1−6 and TMHs 7−12 in ABCB1, respectively. The conserved S289 and S290 residues in the hotspot at the periplasmic side of TMH 6 and TMH 6′ were substituted with A in SASA MsbA and are colored black. OUT and IN refer to the outside and inside of the cytoplasmic membrane, respectively.

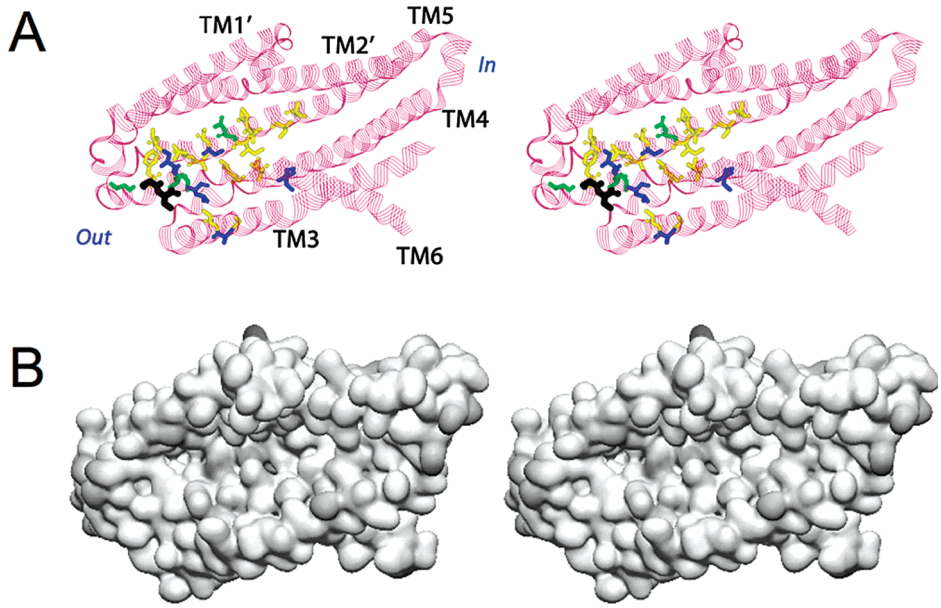

FIGURE 2: Stereoviews of the groove in an MsbA wing. (A) View of TMHs from the dimer interface showing a hotspot of ABCB1 residues implicated in drug binding at the periplasmic side of TMH 6, near the apex of the groove. Color coding and labels are as in the legend of Figure 1. Similar observations can be made for the other wing. (B) Surface representation of the groove formed by the TMHs in panel A.

SASA Mutation Does Not Alter the MsbA-Associated Resistance to Erythromycin but Inhibits the Reversal of Erythromycin Resistance by Taxol. To provide further evidence for the inhibition of Taxol binding by the SASA mutation, the effect of Taxol on erythromycin resistance conferred by Wt or mutant MsbA was studied in cytotoxicity assays. Before this experiment was carried out, the influence of the SASA mutation on MsbA-mediated erythromycin resistance itself was tested (Figure 4A). The concentrations of erythromycin at which cell growth was inhibited by 50% (IC_{50} values) for cells expressing Wt MsbA or the SASA mutant were not affected by this mutation (IC_{50} for Wt MsbA of 0.33 ± 0.03 μM and for the SASA mutant of 0.30 ± 0.02 μM vs an IC_{50} for the nonexpressing control of 60 ± 10 nM). When the experiment was repeated in the presence of increasing amounts of Taxol, approximately 25 μM Taxol was sufficient to reverse the erythromycin resistance of Wt MsbA-expressing cells down to the nonexpressing control, whereas 45 μM Taxol was required for SASA MsbA-expressing cells (Figure 4B), indicating a reduced affinity of SASA MsbA for Taxol. It is important to note that the addition of up to 50 μM Taxol or 2% of the solvent ethanol had no effect on the growth of the cells in the absence of erythromycin.

SASA Mutation Does Not Alter the Interaction of MsbA with Hoechst 33342 but Reduces the Level of Inhibition of MsbA-Mediated Hoechst 33342 Transport by Taxol. The effect of the SASA mutation on taxol binding by MsbA was also examined in Hoechst 33342 binding and transport assays. First, the ability of SASA MsbA and Wt MsbA to interact with Hoechst 33342 was compared. The level of binding of Hoechst 33342 to equimolar amounts of affinity-purified protein was measured by fluorescence at stepwise increasing concentrations of Hoechst 33342. The Hoechst 33342 fluorescence was corrected for nonspecific binding and was then plotted versus the Hoechst 33342 concentration (Figure 5A). Fitting of the data to a hyperbola yielded R^2 values of 0.996 for Wt and 0.988 for SASA MsbA. No significant differences were observed between the binding parameters for Wt MsbA and SASA MsbA (for Wt MsbA, B_{max} = 33.3 ± 1.8 au and K_d = 0.25 ± 0.01 μM; for SASA MsbA, B_{max} = 32.1 ± 1.5 au and K_d = 0.21 ± 0.02 μM). MsbA-dependent Hoechst 33342 transport in inside-out membrane vesicles was studied at various concentrations of Hoechst 33342 to test the effect of the SASA mutation on Hoechst 33342 transport. After subtraction of the values obtained for the control membrane vesicles without MsbA, the transport rates were plotted against the concentration of Hoechst 33342 (Figure 5B). The data for Wt MsbA and SASA MsbA were fitted to a hyperbola with R^2 values of 0.996 and 0.988, respectively, giving a V_{max} of 0.30 ± 0.03 au/s and a K_t of 0.20 ± 0.05 μM for Wt MsbA and a V_{max} of 0.28 ± 0.04 au/s and a K_t of 0.25 ± 0.03 μM for SASA MsbA. Taken together, these results demonstrate that the SASA mutation does not significantly affect the interaction of MsbA with Hoechst 33342.

The effect of Taxol on Hoechst 33342 transport by MsbA Wt was analyzed using inside-out membrane vesicles with or without expressed MsbA. The inside-out membrane vesicles were incubated in the presence of various concentrations of Taxol before 0.25 μM Hoechst 33342 was added, and transport was initiated by the addition of 1 mM ATP. Transport of Hoechst 33342 by Wt MsbA was strongly inhibited at 10 μM Taxol and completely abolished in the presence of 25 μM Taxol, while the activity of SASA MsbA was only weakly affected (Figure 5C,D). To study the type of inhibition underlying this result for Wt MsbA, the kinetics of MsbA-mediated Hoechst 33342 transport were determined in the presence of 10 and 25 μM Taxol (Figure 5E). The resulting Lineweaver−Burk plot points to noncompetitive inhibition of Hoechst 33342 transport by Taxol with an apparent inhibition constant (K_i) of 6.6 ± 1.5 μM Taxol (Figure 5E), which is in the same range as the average K_d (approximately 17 μM) obtained for Taxol binding to MsbA (Figure 3B). Hence, Taxol and Hoechst 33342 most likely interact with MsbA via nonoverlapping binding sites. This conclusion was consistent with the observation that the K_d

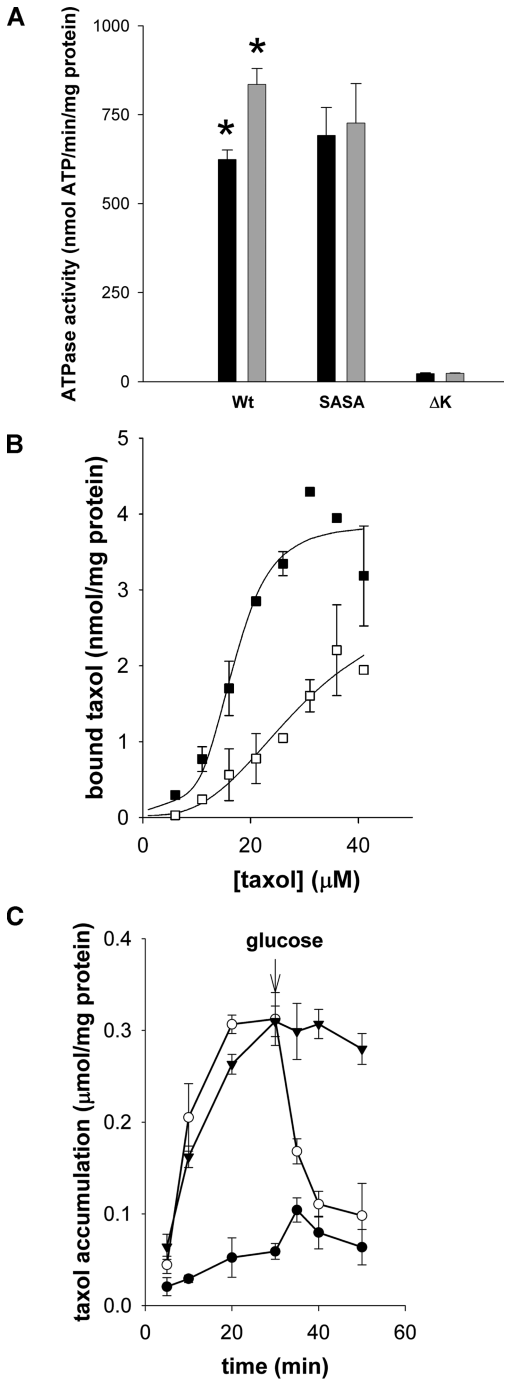

FIGURE 3: SASA mutation impairs the interaction of MsbA with Taxol. (A) SASA mutation inhibits the stimulation of the MsbA ATPase activity in the presence of 25 μM Taxol (black and gray bars, without or with Taxol, respectively). The basal ATPase activity of MsbA is abolished by deletion of the catalytic lysine residue (ΔK382) in the Walker A region (ΔK). The asterisks denote a probability of less than 1% that the difference observed between the mean ATPase activities of Wt MsbA in the absence and presence of Taxol could occur by chance (P value < 0.01). (B) SASA mutation reduces the binding affinity of MsbA for [^{14}C]Taxol. Inside-out membrane vesicles containing MsbA (■) or SASA MsbA (□) were incubated with [^{14}C]Taxol at the indicated concentrations, after which drug binding was assessed by rapid filtration. (C) SASA mutation strongly reduced the rate of active efflux of [^{14}C]Taxol in intact cells. ATP-depleted control cells (●) and cells expressing Wt MsbA (○) or the SASA mutant (▼) were incubated in the presence of 25 μM [^{14}C]Taxol. After 30 min, 25 mM glucose was added (arrow) as a source of metabolic energy, and the amount of cell-associated Taxol was determined by rapid filtration. All values represent the means ± standard error of five independent experiments.

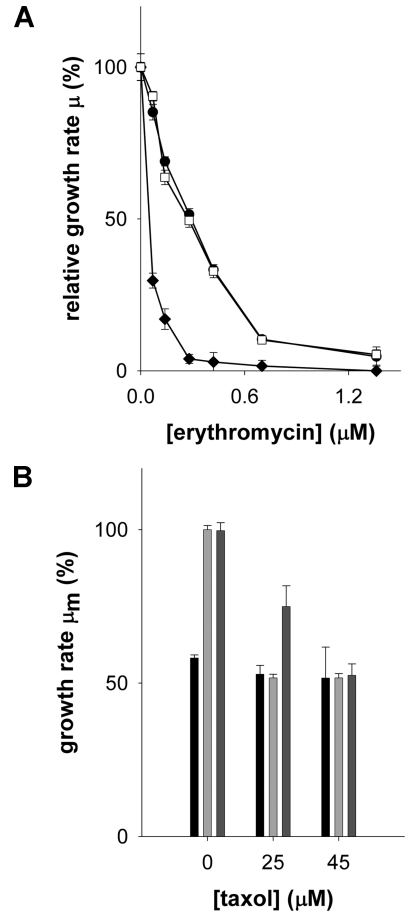

FIGURE 4: SASA mutation does not affect MsbA-mediated erythromycin resistance but inhibits reversal by Taxol. (A) MsbA-mediated erythromycin resistance is not affected by the SASA mutation. Control cells (◆) and cells expressing Wt MsbA (●) or the SASA mutant (□) were grown at 30 °C at increasing concentrations of erythromycin. The specific growth rate (μ_m) was determined at each erythromycin concentration. The μ_m values without antibiotic for Wt MsbA-expressing cells, cells expressing the SASA mutant, and control cells were 0.427 ± 0.012 h^{-1}, 0.431 ± 0.014 h^{-1}, and 0.482 ± 0.008 h^{-1}, respectively, and were set at 100%. (B) Erythromycin resistance conferred by SASA MsbA is less susceptible to reversal by Taxol. Control cells (black) and cells expressing Wt MsbA (light gray) or SASA MsbA (dark gray) were grown in the presence of 0.14 μM erythromycin and increasing concentrations of Taxol. The μ_m of cells expressing Wt MsbA in the absence of Taxol was set at 100%. The addition of up to 50 μM Taxol or 2% of the solvent ethanol had no effect on the μ_m of these cells when they were grown in the absence of erythromycin. In this case, the μ_m was 0.425 ± 0.009 h^{-1} in the presence of 2% ethanol and 0.421 ± 0.011 h^{-1} in the presence of 50 μM Taxol (with 2% ethanol). All values represent the means ± the standard error of five independent experiments.

and B_{max} values for equilibrium binding of Hoechst 33342 to MsbA (see above, Figure 5A) were not significantly altered in the presence of 30 μM Taxol (for Wt MsbA, $B_{max} = 33.0 \pm 0.4$ au and $K_d = 0.24 \pm 0.03$ μM; for SASA MsbA, $B_{max} = 32.9 \pm 4.5$ au and $K_d = 0.21 \pm 0.03$ μM) or in the presence of the solvent (ethanol) control (for Wt MsbA, $B_{max} = 32.9 \pm 1.7$ au and $K_d = 0.19 \pm 0.01$ μM; for SASA MsbA, $B_{max} = 34.7 \pm 1.6$ au and $K_d = 0.24 \pm 0.02$ μM).

SASA MsbA Is Affected in the Binding and Transport of Ethidium. The possible effects of the SASA mutation on the interaction of MsbA with ethidium were studied in equilibrium binding assays based on fluorescence anisotropy. The diffusional rotation of protein-bound ethidium is slower, and

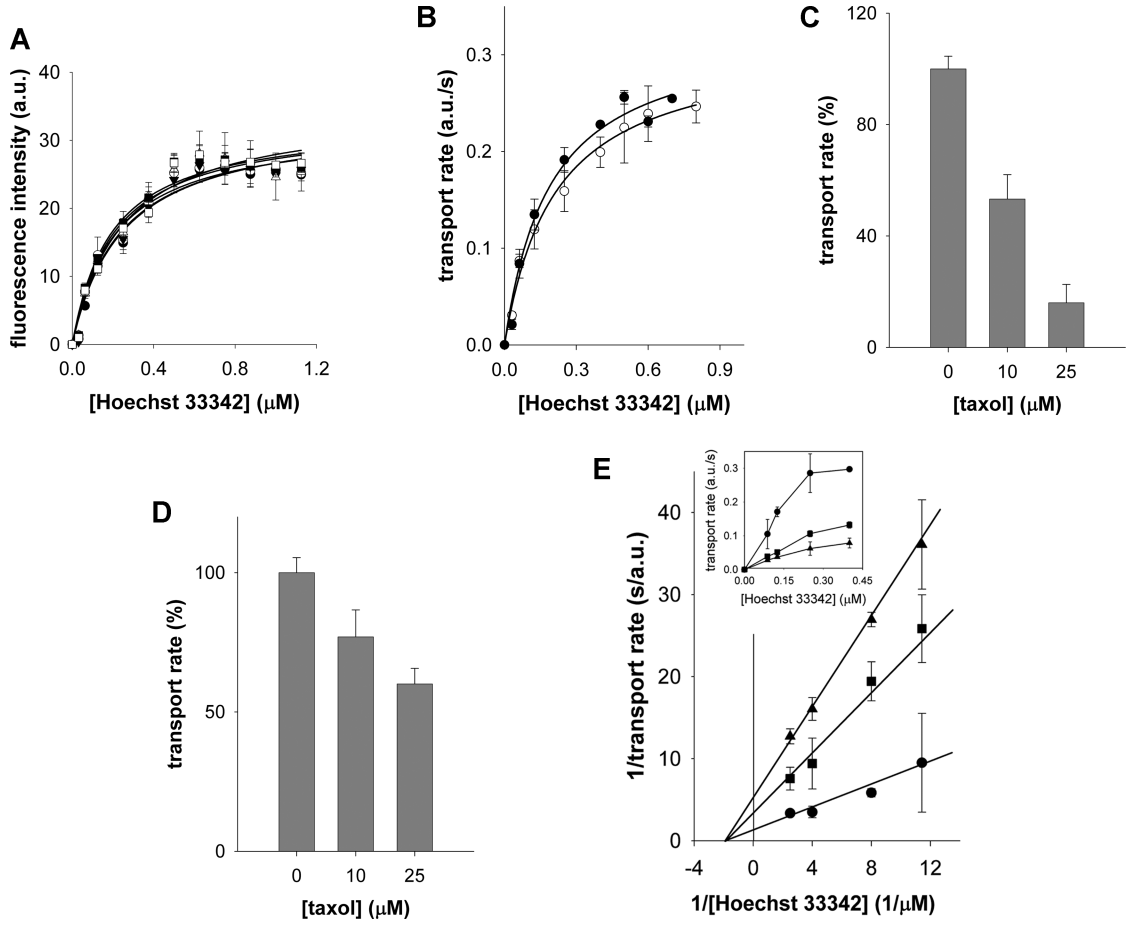

FIGURE 5: SASA mutation does not affect Hoechst 33342 binding and transport by MsbA but reverses the inhibition of Hoechst 33342 transport by Taxol. (A) Hoechst 33342 binding to purified MsbA proteins was assessed by fluorescence spectroscopy in the absence or presence of 50 μM Taxol or its solvent (1% of the total reaction volume): Wt MsbA (●), SASA MsbA (○), Wt MsbA with Taxol (▼), SASA MsbA with Taxol (△), Wt MsbA with solvent (■), and SASA MsbA with solvent (□). (B) Rates of Hoechst 33342 transport by Wt MsbA (●) and SASA MsbA (○) in inside-out membrane vesicles as a function of Hoechst 33342 concentration. All values represent the means ± the standard error of four independent experiments (n = 4). (C) Inhibition by Taxol of Wt MsbA-mediated Hoechst 33342 transport in inside-out membrane vesicles. The rates for transport in the presence of solvent without Taxol (ethanol, 1% of the total reaction volume) were set as 100%. (D) Inhibition by Taxol of MsbA-mediated Hoechst 33342 transport is weakened by the SASA mutation. Hoechst 33342 transport was assessed as described for panel C. (E) Kinetic analysis of Wt MsbA-mediated Hoechst 33342 transport. The initial rates of transport in inside-out membrane vesicles at a range of Hoechst 33342 concentrations were determined in the presence of fixed concentrations of Taxol [(■) 10 and (▲) 25 μM] or the solvent control (●). Inset, rate of Hoechst 33342 transport vs Hoechst 33342 concentration shows the decrease in V_{max} at increasing concentrations of Taxol.

hence, an increase in polarized light emission can be observed upon irradiation with polarized excitation light. When ethidium was titrated with purified Wt MsbA or SASA MsbA protein, a saturable increase in anisotropy was observed. The data could be fitted to a hyperbola (R^2 values of 0.948 for Wt MsbA and 0.941 for SASA MsbA) (Figure 6A), yielding a K_d value for the SASA mutant which was 8-fold higher than the K_d for the Wt protein (K_d = 256.2 ± 47.2 nM for SASA MsbA vs 32.2 ± 5.8 nM for Wt MsbA), and maximum values for the anisotrophy which were comparable (0.131 ± 0.034 for SASA MsbA vs 0.122 ± 0.021 for Wt MsbA). Hence, SASA MsbA has a significantly lower affinity for ethidium than Wt MsbA in these binding assays.

As a reduced level of binding of ethidium to the SASA mutant could have an impact on ethidium transport by the mutant, facilitated uptake and active efflux of ethidium were studied in control cells and cells expressing Wt MsbA or SASA MsbA. In addition to SASA MsbA, a mutant MsbA protein was included in these experiments in which catalytic lysine residue 382 in the Walker A sequence of the nucleotide-binding domain (NBD) was deleted. Consistent with previous observations on the ΔK388 mutant of LmrA (*15*), MsbA ΔK382 lacks significant ATPase activity (Figure 3A). When the cells had been preloaded with ethidium, those expressing the ΔK382 mutant did not exhibit a significant efflux activity compared to the control (efflux rate of 0.011 ± 0.006 au/s for ΔK382 MsbA vs 0.001 ± 0.003 au/s for the control), whereas the SASA mutant exhibited a significantly lower level of ethidium efflux than the cells expressing Wt MsbA (efflux rate of 0.091 ± 0.006 au/s for SASA MsbA vs 0.156 ± 0.008 au/s for Wt MsbA) (Figure 6B).

Ethidium accumulation experiments using ATP-depleted control cells and cells expressing Wt MsbA, SASA MsbA, or ΔK382 MsbA revealed that the cells expressing the SASA mutant accumulated more ethidium than control cells or cells expressing ΔK382 MsbA, but that the rate of uptake was reduced in comparison to that of cells expressing the Wt protein (uptake rate of 0.111 ± 0.008 au/s for SASA MsbA vs 0.150 ± 0.011 au/s for Wt MsbA, 0.088 ± 0.007 au/s for ΔK382 MsbA, and 0.053 ± 0.005 au/s for the nonexpressing control) (Figure 6C). To further test the validity of this

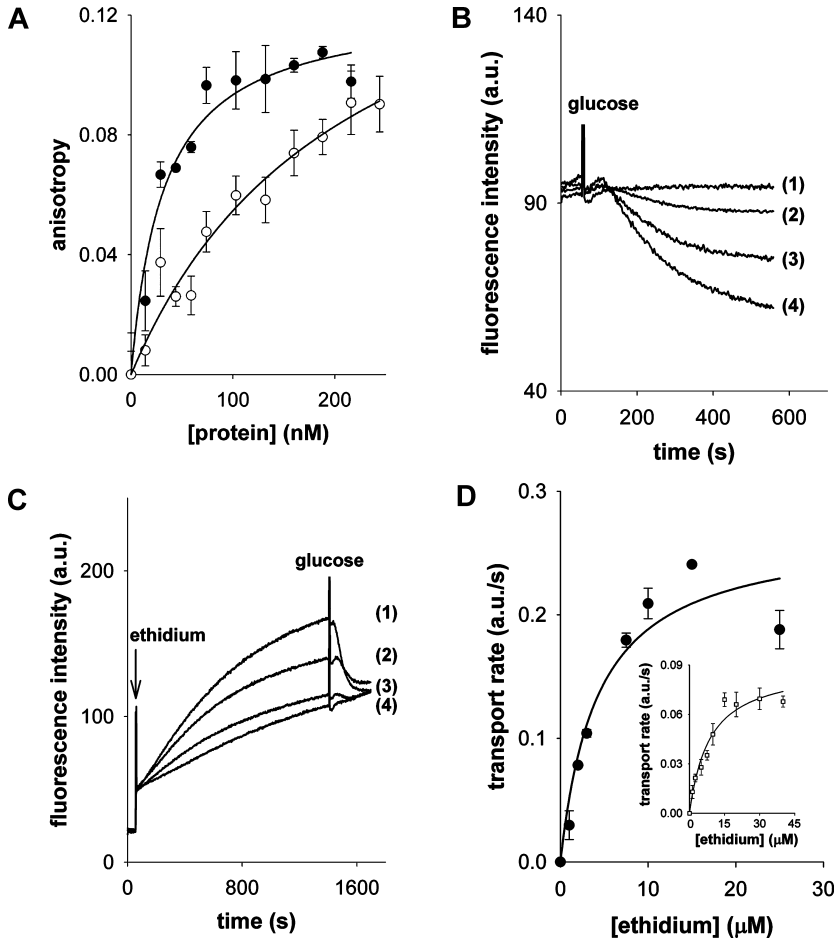

FIGURE 6: Ethidium binding and transport by MsbA are inhibited by the SASA mutation. (A) Ethidium binding to purified protein was assessed by fluorescence anisotropy. Purified Wt MsbA (●) and the SASA mutant (○) were used to titrate 1 μM ethidium, and the changes in fluorescence anisotropy were recorded. (B) MsbA-mediated extrusion of ethidium is inhibited by the SASA mutation. Cells without MsbA expression (control) (trace 1) or with expression of ΔK382 MsbA (trace 2), SASA MsbA (trace 3), or Wt MsbA (trace 4) were preloaded in the presence of 2 μM ethidium. Energy-dependent ethidium efflux was initiated by the addition of 25 mM glucose. (C) SASA mutation inhibits MsbA-mediated ethidium uptake in ATP-depleted cells. Ethidium (2 μM) (arrow) was added to ATP-depleted cells expressing Wt MsbA (trace 1), SASA MsbA (trace 2), ΔK382 MsbA (trace 3), or no MsbA (trace 4). Ethidium uptake was recorded until a steady state was reached. Glucose (25 mM) was then added to initiate active ethidium efflux by MsbA. (D) Kinetic analysis of ethidium uptake by Wt MsbA (main panel) and the SASA mutant (inset). Initial rates of uptake of ethidium into control cells or cells expressing Wt MsbA or SASA MsbA were determined over the first 100 s of linear uptake. The rates obtained for control cells were subtracted, and the data were plotted vs ethidium concentration. All values represent the means ± the standard error of five independent experiments.

observation, ethidium uptake was assessed over a range of ethidium concentrations. The initial linear rates of transport were plotted against the ethidium concentration, and the data were fitted to a hyperbola with an R^2 of 0.951 (Figure 6D), yielding a V_{max} of 0.24 ± 0.03 au/s and a K_t of 2.6 ± 0.4 μM for Wt MsbA and a V_{max} of 0.08 ± 0.01 au/s and a K_t of 8.1 ± 0.4 μM for SASA MsbA. Hence, similar to the ethidium binding experiments, the ethidium transport measurements indicated a reduction in the apparent affinity of SASA MsbA for ethidium. In addition, the SASA mutant exhibited a reduced maximum rate of ethidium transport.

DISCUSSION

One of the interesting aspects of multidrug transporters relates to the question of how these systems recognize structurally diverse drug substrates. Many attempts have been made in the past 18 years to identify the positions of drug binding sites in ABCB1. In a recent analysis of published mutations in ABCB1 that influence drug transport and/or drug resistance in intact cells, we separated change-in-specificity mutations that affect the specificity for individual substrates from those that either modify the expression of the protein at the cell surface or alter the overall transport mechanism, both determined by a comparable change in the transport of all substrates tested (*9*). As a high-resolution, three-dimensional structure of ABCB1 is not yet available, we superimposed these residues from this study on the crystal structure of the bacterial ABCB1 homologue MsbA from *S. typhimurium* (*10*) that shares similarity with the structure of Sav1866 (*11*). Interestingly, we observed the colocalization of the change-in-specificity mutations in TMH 5′, and in a hotspot at the periplasmic side of TMH 6 and TMH 6′ (Figures 1 and 2). The change-in-specificity mutations also colocalized with residues in ABCB1 implicated in the binding of thiol-reactive drug analogues in cysteine scanning mutagenesis experiments (*9, 22, 23*) (Figures 1 and 2). The positions of these residues are consistent with photoaffinity labeling and mass spectrometry experiments on ABCB1, which have implicated TMH 5 and 6 and TMH 8, 11, and 12 in the binding of a number of affinity ligands, including iodomycin, iodipine, azidopine, IAAP, AIIP-forskolin, propafenones, and taxanes, though not all substrates have been

demonstrated to bind to all regions in both half-transporters (reviewed in ref *24*).

E. coli MsbA is known to interact with multiple ABCB1 substrates (*5–8*), but key regions affecting drug−protein interactions in this bacterial ABC transporter have not yet been identified. To test the possible role of TMH 6 in drug binding and transport by MsbA, we generated the SASA mutation in the predicted hotspot in TMH 6 and TMH 6′. SASA MsbA was as well expressed as Wt MsbA. The mutation did not significantly change the interactions of MsbA with Hoechst 33342 in equilibrium binding and transport assays (Figure 5A,B) or the interaction with erythromycin in a cytotoxicity assay (Figure 4A). However, SASA MsbA did exhibit a change in the interaction with Taxol. In an equilibrium binding assay with [^{14}C]Taxol, the mutant exhibited a significantly reduced affinity for Taxol (Figure 3B). The mutant failed to exhibit a Taxol-stimulated ATPase activity (Figure 3A) and exhibited a strongly reduced rate of active efflux of this substrate in intact cells compared to Wt MsbA (Figure 3C). The SASA mutation also reversed the Taxol-dependent inhibition of Hoechst 33342 transport and the Taxol-dependent reversal of erythromycin resistance (Figures 4B and 5C,D). The interaction of purified MsbA with ethidium in fluorescence anisotropy experiments was significantly reduced for the mutant (Figure 6A). Both the facilitated influx of ethidium and the active efflux of ethidium were significantly reduced for the mutant (Figure 6B−D). As the SASA mutation alters the transport and binding of ethidium and Taxol but does not affect the interactions with Hoechst 33342 and erythromycin, SASA MsbA exhibits a change-in-specificity phenotype similar to that of the change-in-specificity mutants of ABCB1 on which the identification of the hotspot region in TMH 6 and TMH 6′ of MsbA was based.

Our observations share similarities with studies of the resistance-nodulation-cell division (RND) type of efflux systems in Gram-negative bacteria. AcrB from *E. coli* is the best-characterized member of this family and functions in a complex with two accessory proteins, TolC and AcrA, to export a wide variety of substrates (*25, 26*). Crystallographic analyses of AcrB have recently shown that the protein forms an asymmetric trimer in which each protomer contains a binding chamber in its periplasmic domain for the antibiotics minocycline and doxorubicin (*25, 26*). Mutational analyses of the *E. coli* AcrB homologues MexD from *Pseudomonas aeruginosa* (*27*), AcrB from *Haemophilus influenza* (*28*), and MdtF from *E. coli* (*29*) have indicated that substitutions of residues (Q34K, P328L, and F608S in MexD, A288C in $AcrB_{HI}$, and V610F in MdtF) close to or within the binding chamber increase the rate of transport of a given drug while decreasing or not affecting the rate of transport of another, similar to the phenotype of the change-in-specificity mutations in ABCB1 and the SASA mutant in *E. coli* MsbA. Comparable observations have been published for multidrug-binding transcriptional regulators such as BmrR from *Bacillus subtilis* and QacR from *St. aureus*, where mutations in the multidrug binding pocket affected the binding affinity of a variety of ligands differently (*30, 31*). It is noteworthy that although the SASA mutation inhibits interactions of MsbA with ethidium and the antimitotic drug Taxol, Taxol itself did not directly inhibit the binding or the transport of ethidium by Wt MsbA (data not shown), suggesting that both substrates might bind simultaneously to a common surface in MsbA. The structural mechanism of the simultaneous binding of two drugs to a multidrug-binding protein has been resolved for QacR, for which it was found that simple structural changes induced by binding of one ligand can explain seemingly complicated biochemical behavior for the binding of the second ligand to the same surface (*31*). Consistent with this, our previous studies on drug interactions in MsbA indicated that another antimitotic drug, vinblastine, directly competes with ethidium for binding to MsbA (*6*). Taken together, the results support the notion that the periplasmic sides of TMH 6 and TMH 6′ in dimeric MsbA contribute to a binding surface for drugs, which might utilize similar principles for drug binding as established for QacR and AcrB.

In our structural comparisons of ABCB1 and MsbA, we used the structure of the ATP-bound, outward-facing conformation of MsbA (*10*). The observation that change-in-specificity mutations and residues in ABCB1 accessible to thiol-reactive drugs colocalize at the periplasmic side of TMH 6 and TMH 6′ in a major groove in each of the two wings of MsbA in which their exposure is limited is consistent with the notion that this protein conformation promotes the release of drugs to the external environment. In contrast, in the V-shaped, inward-facing conformation of apo MsbA (*10*), the periplasmic sides of TMH 6 and TMH 6′ are in the proximity of each other at the top of the chamber formed between both half-transporters, where they are exposed to the chamber. In this conformation, these helical regions could promote drug binding from the interior. Recent pulse double electron−electron resonance and fluorescence homo transfer experiments have provided evidence for the ATP hydrolysis-dependent conformational motion of dimeric MsbA between the inward-facing and outward-facing conformations (*32*). It is interesting to note that a V-shaped, inward conformation has also been observed for the two MDs in the crystallized 2×6 TMH-containing molybdate importer ($ModB_2C_2$) from *Archaeoglobus fulgidus* (*33*). As the cytoplasmic extensions of TMH 6 and TMH 6′ in dimeric MsbA (in the intracellular domains, see Figure 1) are directly linked to the NBDs, these helices might provide a crucial link between ATP binding/hydrolysis and drug binding/dissociation in MsbA. Our observations are the first to demonstrate the importance of TMH 6 in the MsbA monomers in the binding and translocation of multiple drugs.

ACKNOWLEDGMENT

H.W.V.V. would like to thank B.W. and past and present laboratory members for their enthusiasm and input during the 3 years of experimental work underlying this paper. We appreciate discussions with Geoffrey Chang and Kaspar Locher, and thank Peter Henderson for the kind gift of GalP-containing membrane vesicles. Daniel Gutmann is acknowledged for critical reading of the manuscript.

REFERENCES

1. Higgins, C. F. (2007) Multiple molecular mechanisms for multidrug resistance transporters. *Nature 446*, 749–757.
2. Borst, P., and Elferink, R. O. (2002) Mammalian ABC transporters in health and disease. *Annu. Rev. Biochem. 71*, 537–592.
3. Doerrler, W. T. (2006) Lipid trafficking to the outer membrane of Gram-negative bacteria. *Mol. Microbiol. 60*, 542–552.

4. Doerrler, W. T., Reedy, M. C., and Raetz, C. R. (2001) An *Escherichia coli* mutant defective in lipid export. *J. Biol. Chem. 276*, 11461–11464.
5. Reuter, G., Janvilisri, T., Venter, H., Shahi, S., Balakrishnan, L., and Van Veen, H. W. (2003) The ATP binding cassette multidrug transporter LmrA and lipid transporter MsbA have overlapping substrate specificities. *J. Biol. Chem. 278*, 35193–35198.
6. Woebking, B., Reuter, G., Shilling, R. A., Velamakanni, S., Shahi, S., Venter, H., Balakrishnan, L., and Van Veen, H. W. (2005) Drug-lipid A interactions on the *Escherichia coli* ABC transporter MsbA. *J. Bacteriol. 18*, 6363–6369.
7. Ghanei, H., Abeyrathne, P. D., and Lam, J. S. (2007) Biochemical characterization of MsbA from *Pseudomonas aeruginosa*. *J. Biol. Chem. 282*, 26939–26947.
8. Eckford, P. D., and Sharom, F. J. (2008) Functional characterization of *E. coli* MsbA: Interaction with nucleotides and substrates. *J. Biol. Chem. 283*, 12840–12850.
9. Shilling, R. A., Venter, H., Velamakanni, S., Bapna, A., Woebking, B., Shahi, S., and Van Veen, H. W. (2006) New light on multidrug binding by an ATP-binding-cassette transporter. *Trends Pharmacol. Sci. 27*, 195–203.
10. Ward, A., Reyes, C. L., Yu, J., Roth, C. B., and Chang, G. (2007) Flexibility in the ABC transporter MsbA: Alternating access with a twist. *Proc. Natl. Acad. Sci. U.S.A. 104*, 19005–19010.
11. Dawson, R. J., and Locher, K. P. (2006) Structure of a bacterial multidrug ABC transporter. *Nature 443*, 180–185.
12. Rosenberg, M. F., Callaghan, R., Modok, S., Higgins, C. F., and Ford, R. C. (2005) Three-dimensional structure of P-glycoprotein: The transmembrane regions adopt an asymmetric configuration in the nucleotide-bound state. *J. Biol. Chem. 280*, 2857–2862.
13. De Ruyter, P. G., Kuipers, O. P., and De Vos, W. M. (1996) Controlled gene expression systems for *Lactococcus lactis* with the food-grade inducer nisin. *Appl. Environ. Microbiol. 62*, 3662–3667.
14. Lubelski, J., De Jong, A., Van Merkerk, R., Agustiandari, H., Kuipers, O. P., Kok, J., and Driessen, A. J. (2006) LmrCD is a major multidrug resistance transporter in *Lactococcus lactis*. *Mol. Microbiol. 61*, 771–781.
15. Venter, H., Velamakanni, S., Balakrishnan, L., and Van Veen, H. W. (2008) On the energy-dependence of Hoechst 33342 transport by the ABC transporter LmrA. *Biochem. Pharmacol. 75*, 866–874.
16. Margolles, A., Putman, M., Van Veen, H. W., and Konings, W. N. (1999) The purified and functionally reconstituted multidrug transporter LmrA of *Lactococcus lactis* mediates the transbilayer movement of specific fluorescent phospholipids. *Biochemistry 38*, 16298–16306.
17. Van Veen, H. W., Margolles, A., Muller, M., Higgins, C. F., and Konings, W. N. (2000) The homodimeric ATP-binding cassette transporter LmrA mediates multidrug transport by an alternating two-site (two-cylinder engine) mechanism. *EMBO J. 19*, 2503–2514.
18. Gutmann, D. A. P., Mizohata, E., Newstead, S., Ferrandon, S., Postis, V., Xia, X., Henderson, P. J. F., Van Veen, H. W., and Byrne, B. (2007) A high-throughput method for membrane protein solubility screening: The ultracentrifugation dispersity sedimentation assay. *Protein Sci. 16*, 1422–1428.
19. Bapna, A., Federici, L., Venter, H., Velamakanni, S., Luisi, B., Fan, T. P., and Van Veen, H. W. (2007) Two proton translocation pathways in a secondary-active multidrug transporter. *J. Mol. Microbiol. Biotechnol. 12*, 197–209.
20. Velamakanni, S., Janvilisri, T., Shahi, S., and Van Veen, H. W. (2008) A functional steroid-binding element in an ATP-binding cassette multidrug transporter. *Mol. Pharmacol. 73*, 12–17.
21. Glasfeld, A., Koehler, A. N., Schumacher, M. A., and Brennan, R. G. (1999) The role of lysine 55 in determining the specificity of the purine repressor for its operators through minor groove interactions. *J. Mol. Biol. 291*, 347–361.
22. Loo, T. W., and Clarke, D. M. (2001) Defining the drug-binding site in the human multidrug resistance P-glycoprotein using a methanethiosulfonate analog of verapamil, MTS-verapamil. *J. Biol. Chem. 276*, 14972–14979.
23. Loo, T. W., and Clarke, D. M. (2002) Location of the rhodamine-binding site in the human multidrug resistance P-glycoprotein. *J. Biol. Chem. 277*, 44332–44338.
24. Peer, M., Csaszar, E., Vorlaufer, E., Kopp, S., and Chiba, P. (2005) Photoaffinity labeling of P-glycoprotein. *Mini Rev. Med. Chem. 5*, 165–172.
25. Murakami, S., Nakashima, R., Yamashita, E., Matsumoto, T., and Yamaguchi, A. (2006) Crystal structures of a multidrug transporter reveal a functionally rotating mechanism. *Nature 443*, 173–179.
26. Seeger, M. A., Schiefner, A., Eicher, T., Verrey, F., Diederichs, K., and Pos, K. M. (2006) Structural asymmetry of AcrB trimer suggests a peristaltic pump mechanism. *Science 313*, 1295–1298.
27. Mao, W., Warren, M. S., Black, D. S., Satou, T., Murata, T., Nishino, T., Gotoh, N., and Lomovskaya, O. (2002) On the mechanism of substrate specificity by resistance nodulation division (RND)-type multidrug resistance pumps: The large periplasmic loops of MexD from *Pseudomonas aeruginosa* are involved in substrate recognition. *Mol. Microbiol. 46*, 889–901.
28. Dastidar, V., Mao, W., Lomovskaya, O., and Zgurskaya, H. I. (2007) Drug-induced conformational changes in multidrug efflux transporter AcrB from *Haemophilus influenzae*. *J. Bacteriol. 189*, 5550–5558.
29. Bohnert, J. A., Schuster, S., Fähnrich, E., Trittler, R., and Kern, W. V. (2007) Altered spectrum of multidrug resistance associated with a single point mutation in the *Escherichia coli* RND-type MDR efflux pump YhiV (MdtF). *J. Antimicrob. Chemother. 59*, 1216–1222.
30. Vazquez-Laslop, N., Markham, P. N., and Neyfakh, A. A. (1999) Mechanism of ligand recognition by BmrR, the multidrug-responding transcriptional regulator: Mutational analysis of the ligand-binding site. *Biochemistry 38*, 16925–16931.
31. Schumacher, M. A., Miller, M. C., and Brennan, R. G. (2004) Structural mechanism of the simultaneous binding of two drugs to a multidrug-binding protein. *EMBO J. 23*, 2923–2930.
32. Borbat, P. P., Surendhran, K., Bortolus, M., Zou, P., Freed, J. H., and Mchaourab, H. S. (2007) Conformational motion of the ABC transporter MsbA induced by ATP hydrolysis. *PLoS Biol. 5*, e271.
33. Hollenstein, K., Frei, D. C., and Locher, K. P. (2007) Structure of an ABC transporter in complex with its binding protein. *Nature 446*, 213–216.

BI800778D